Carbonization Kinetics of Various Biomass Sources

Didem Özçimen[1,*] and Ayşegül Ersoy-Meriçboyu[2]

[1]*Yıldız Technical University, Faculty of Chemical and Metallurgical Engineering, Bioengineering Department, Esenler 34201, Istanbul, Turkey*

[2]*Istanbul Technical University, Chemical-Metallurgical Engineering Faculty, Department of Chemical Engineering, Maslak 34469, Istanbul, Turkey*

Abstract: Hazelnut shell, apricot stone, grapeseed and chestnut shell samples were carbonized in a thermogravimetric (TG) analyzer at different conditions to determine the carbonization kinetic parameters. Three different calculation methods and 22 different model equations concerning solid-state rate controlling mechanisms were used for the kinetic analysis of the carbonization TG curves. A computer program in BASIC which enables regression analysis, was used to calculate the kinetic parameters from experimental TG data. It was observed that the different values of Arrhenius parameters (E and Log A) were obtained depending on the method of calculation, the gaseous atmosphere and the sample properties. The most appropriate kinetic model which represents the carbonization of the cellulosic and lignin ingredients of the biomass samples were found as $f(\alpha)=(1-\alpha)^2$ and $f(\alpha)=0.5\cdot(1-\alpha)\cdot[-\ln(1-\alpha)]^{-1}$, respectively.

Keywords: Carbonization kinetics, hazelnut shell, apricot stone, grapeseed, chestnut shell.

1. INTRODUCTION

As known, the usage of renewable energy sources is very important due to the depletion of fossil fuels, global warming and the environmental pollution. In this context, biomass is considered as an important alternative energy source. In order to convert biomass sources into more useful forms, thermochemical conversion processes such as carbonization, pyrolysis and gasification are widely applied. To design appropriate systems for these processes, having a knowledge of the process kinetics is required. Thermoanalytical methods are often used for the kinetic analysis of solid-phase thermal decomposition reactions. During carbonization total weight loss of the sample depending on parallel and sequential thermal can be measured by thermogravimetric analysis as a function of time and temperature [m=f (t or T)]. In this way, thermogravimetric analysis results give general information on the overall reaction kinetics, not the individual reactions [1-3].

It is known that many parallel and consecutive reactions occur during the carbonization of biomass sources. The kinetic parameters of the process also vary in this complex reaction system according to these reactions and various interactions. Biomass resources which have lignocellulosic composition comprise complex structures such as cellulose, hemicellulose, lignin, water, extractives and mineral matters. Generally, three main components of biomass that are hemicellulose, cellulose and lignin decompose at different temperatures due to their different molecular structures [4]. Although the thermal decomposition mechanisms of these components are not well known completely, several studies relating with the thermal decomposition mechanisms of cellulose, hemicellulose and lignin were reported in the literature [5-7]. The common point of these studies is that experimental TG data were used to calculate the kinetic parameters.

Orfao and Figueiredo studied the pyrolysis kinetics of pine and eucalyptus wood chips, and pine bark samples. It was reported that the different activation energy and frequency multiplier values were found for the decomposition of hemicellulose, cellulose and lignin components of the samples [8]. Similar to this study, the pyrolysis kinetics of three different wood species (pine, walnut shell and carob) [9]; rice husk [10]; almond and walnut shell and beech wood [11]; cherry stones [12]; wood and cotton waste [13]; seaweeds and firewood [14]; date palm [15]; wood pellets [16]; hazelnut husk [17] were investigated *via* thermogravimetric technique. In these studies it was concluded that the cellulosic and lignin components of biomass samples were broken down independently from each other and the values of the kinetic parameters (activation energy, reaction order and rate constant) representing thermal decomposition of cellulosic and lignin components were also showed differences depending on the sample properties.

In this study, the carbonization kinetics of various biomass samples such as apricot stone, hazelnut shell, grapeseed and chestnut shell were investigated by using of non-isothermal thermogravimetric technique.

*Address correspondence to this author at the Yıldız Technical University, Faculty of Chemical and Metallurgical Engineering, Bioengineering Department, Esenler 34210, Istanbul, Turkey; Tel: +90 212 383 4635;
Fax: 0212 383 4625; E-mail: ozcimen@yildiz.edu.tr

E-ISSN: 2409-983X/14

Kinetic analysis of the carbonization TG curves obtained at different conditions was achieved by applying three different computational methods and the kinetic data were presented comparatively.

2. EXPERIMENTAL

2.1. Materials

The hazelnut shell (*Corylus avellana*) sample obtained from Giresun located in the Black Sea region of Turkey, the apricot stone (*Prunus armeniaca*) sample obtained from Malatya located in the east Anatolian region of Turkey, the grapeseed (*Vitris vinifera*) sample obtained from a vine factory located in the middle Anatolian region of Turkey and the chestnut shell (*Castanea sative mill*) sample obtained from a chestnut candy factory in Bursa located in the Marmara region of Turkey were used in this study. Experiments were performed with air-dried apricot stone and hazelnut shell samples which have the particle sizes of 1–1.4 mm and 0.250-0.355 mm. Since the particles of grapeseed and chestnut shell samples stick to each other during grinding and sieving operations, their particle size range could not be determined precisely. Therefore, standard sieve analysis was applied for grapeseed and chestnut shell samples and their mean average diameters were found as 0,657 mm and 0,377 mm, respectively. So, the grapeseed and chestnut shell samples having the average particle diameter and coarse unpulverized samples with a particle size of higher than 2 mm were used.

2.2. Method

Carbonization experiments were carried out in a Shimadzu TG 41 model thermal analyzer at different conditions and presented in Table **1**. The initial mass of samples used in the measurements was about 40 mg. The experiments were performed from room temperature to 923 K by applying the linear heating rates of 5 and 20 K/min and sweep gas flow rates of 0 cm^3/min (static atmosphere) and 40 cm^3/min (dynamic atmosphere). Pure nitrogen (N_2) was used as sweep gas. Before heating, in order to provide an inert environment, the system was flushed with pure nitrogen for 15 min. A chart speed of 2.5 mm/min was used to trace carbonization TG curves.

Table 1: Carbonization Conditions of Biomass Samples

Experimental code	Material	Heating rate (K/min)	N_2 flow rate (cm^3/min)	Particle size (mm)
H1	Hazelnut shell	5	0	0.250-0.355
H2	Hazelnut shell	20	0	0.250-0.355
H3	Hazelnut shell	5	40	0.250-0.355
H4	Hazelnut shell	20	40	0.250-0.355
H5	Hazelnut shell	5	40	1-1.4
A1	Apricot stone	5	0	0.250-0.355
A2	Apricot stone	20	0	0.250-0.355
A3	Apricot stone	5	40	0.250-0.355
A4	Apricot stone	20	40	0.250-0.355
A5	Apricot stone	5	40	1-1.4
G1	Grapeseed	5	0	0.657
G2	Grapeseed	20	0	0.657
G3	Grapeseed	5	40	0.657
G4	Grapeseed	20	40	0.657
G5	Grapeseed	5	40	>2
C1	Chestnut shell	5	0	0.377
C2	Chestnut shell	20	0	0.377
C3	Chestnut shell	5	40	0.377
C4	Chestnut shell	20	40	0.377
C5	Chestnut shell	5	40	>2

2.3. Theory

Since TG curves are a function of the reaction kinetics, the kinetic parameters including the activation energy, pre-exponential factor and mechanism can be calculated from these curves [18-20]. The methods used to calculate the kinetic parameters are based on the following three equations [19]:

$$\frac{d\alpha}{dt} = k \cdot f(\alpha) \quad (1)$$

$$k = A.\exp\left(\frac{-E}{RT}\right) \quad (2)$$

$$T=T_0+b.t \quad (3)$$

where α is the degree of conversion, T (K) is the temperature at time t, T_0 (K) is initial temperature, k (s^{-1}) is the rate constant, t (s) is time, f(α) is the conversion function which depends on the reaction mechanism, A (s^{-1}) and E ($kJ.mol^{-1}$) are the pre-exponential factor and apparent activation energy, respectively, R ($kJ.mol^{-1}.K^{-1}$) is the gas constant and b ($K.\ s^{-1}$) is the linear heating rate. The normalized degree of conversion can be calculated by the following equation.

$$\alpha = \frac{W_0 - W_t}{W_0 - W_\infty} \quad (4)$$

where W_0 is the sample mass at initial time, W_t is the sample mass at time t and W_∞ is the sample mass at the end of the reaction.

If the equations (1-4) are combined and linearized, equation 5 is obtained.

$$\ln\left[\frac{d\alpha/dT}{f(\alpha)}\right] = \ln\left[\frac{A}{b}\right] - \left[\frac{E}{RT}\right] \quad (5)$$

According to this equation a plot of "ln[(d(α)/dT)/ f(α)]" versus "1/T" should give a straight line if the appropriate f(α) function is selected. Arrhenius parameters (E and A) can be obtained from the slope and intercept, respectively. Equation (5) was used by many researchers to calculate kinetic parameters for different f(α) functions [20-24].

In this study, in order to calculate the carbonization kinetic parameters, calculation methods which are namely Coats–Redfern [22], Dharwadkar–Karkhanavala [25] and Van Krevelen [26] were used. 22 different model equations describing the rate controlling mechanisms of solid state decomposition reactions were applied to determine model equation [f(α)] that best represents the carbonization mechanism. Table **2** lists the differential f(α) and integral expressions g(α) of these models. Carbonization kinetic parameters were determined by a computer program in BASIC which enables regression analysis. As input data for the computer program, the experimental data such as constant heating rate, initial and final sample weights and α–T data which are derived from TG curves were employed. The f(α) functions which yield the highest correlation coefficients and provide reasonably good fitting to the experimental data were determined and used to calculate Arrhenius parameters "E" and "log A".

3. RESULTS AND DISCUSSION

On the carbonization TG curves of all biomass samples, three distinct mass loss regions having different slopes were observed (Figures **1-3**). Since all figures are very similar, only figures for hazelnut shell was given. The first region that corresponds to the moisture release started approximately at 323 K and completed in the temperature interval of 373-433 K depending on the sample type, particle size and carbonization atmosphere. In this region, very little mass loss was observed for all samples. The second region started at the end of this region and a very fast mass loss was detected in this region. This region represents the decomposition of cellulosic components (hemicellulose and cellulose) of samples. The start and end points varied between 433-483 K and 533–623 K in this decomposition, respectively, depending on the sample type, particle size and carbonization atmosphere. After the second region, the third mass loss region which characterizes the thermal decomposition of the lignin component of biomass samples, started where a rather slower mass loss occurs. Unlike the cellulosic components of the samples, lignin decomposes over a wider temperature range as compared to those. The start and end points of third region were altered between 543-633 K and 723-903 K, respectively, depending on the sample properties and the carbonization conditions.

Since the decomposition temperatures, rates, mechanism and pathways of the cellulosic and lignin constituents of the samples are different, various mass loss regions were observed on the carbonization TG curves (Figures **1-3**). It is also known that, different values of kinetic parameters are obtained depending on the differences in TG curves [18]. Therefore, the kinetic parameters were calculated separately for the

Table 2: Model Equations Used in the Kinetic Analysis

Model	Mechanism	Differential function $f(\alpha)$	Integral function $g(\alpha)=\int d(\alpha)/f(\alpha)$
1. First-order eqn. (n=1)	Chemical reaction (Fn1)	$(1-\alpha)$	$-\ln(1-\alpha)$
2. Zero-order eqn. (n=0)	Chemical reaction (Fn 0)	1	α
3.One-third eqn. (n=1/3)	Chemical reaction (Fn 1/3)	$(1-\alpha)^{1/3}$	$3/2.[1-(1-\alpha)^{2/3}]$
4. One-half order eqn. (n=1/2)	Chemical reaction (Fn ½)	$(1-\alpha)^{1/2}$	$2.[1-(1-\alpha)^{1/2}]$
5. Two-thirds order eqn (n=2/3)	Chemical reaction (Fn 2/3)	$(1-\alpha)^{2/3}$	$3.[1-(1-\alpha)^{1/3}]$
6. Second-order eqn. (n=2)	Chemical reaction (Fn 2)	$(1-\alpha)^{2}$	$[1.(1-\alpha)^{-1}]$
7. Third-order eqn. (n=3)	Chemical reaction (Fn 3)	$0.5.(1-\alpha)^{3}$	$[1.(1-\alpha)^{-1}]^{2}$
8. Three-half order eqn. (n=3/2)	Chemical reaction Fn(3/2)	$(1-\alpha)^{3/2}$	$2.[(1-\alpha)^{-1/2}-1]$
9. Phase boundary controlled reaction eqn.	Contraction geometry (cylindrical symmetry) (R2)	$2.(1-\alpha)^{1/2}$	$1-(1-\alpha)^{1/2}$
10. Phase boundary controlled reaction eqn.	Contraction geometry (spherical symmetry) (R3)	$3.(1-\alpha)^{2/3}$	$1-(1-\alpha)^{1/3}$
11. Avrami-Erofeev eqn.	Random nucleation and growth of nuclei (n=1.5), (A1.5)	$1.5.(1-\alpha).[-\ln(1-\alpha)]^{1/3}$	$[-\ln(1-\alpha)]^{2/3}$
12. Avrami-Erofeev eqn.	Random nucleation and growth of nuclei (n=2), (A2)	$2.(1-\alpha).[-\ln(1-\alpha)]^{1/2}$	$[-\ln(1-\alpha)]^{1/2}$
13. Avrami-Erofeev eqn.	Random nucleation and growth of nuclei (n=3), (A3)	$3.(1-\alpha).[-\ln(1-\alpha)]^{2/3}$	$[-\ln(1-\alpha)]^{1/3}$
14. Avrami-Erofeev eqn.	Random nucleation and growth of nuclei (n=4), (A4)	$4.(1-\alpha).[-\ln(1-\alpha)]^{3/4}$	$[-\ln(1-\alpha)]^{1/4}$
15. Valensi Barrer eqn.	Two-dimensional diffusion (D2)	$[-\ln(1-\alpha)]^{-1}$	$\alpha-(1-\alpha).\ln(1-\alpha)$
16. Jander eqn.	Three-dimensional diffusion (spherical symmetry) (D3)	$(3/2).(1-\alpha).^{2/3}[1-(1-\alpha)^{1/3}]^{-1}$	$[1-(1-\alpha)^{1/3}]^{2}$
17. Ginstling-Brounstain eqn.	Three-dimensional diffusion (cylindrical symmetry) (D4)	$(3/2).[1-(1-\alpha)^{1/3}]^{-1}$	$[1-(2/3).\alpha]-(1-\alpha)^{2/3}$
18. Zhuravlev-Lesokhin-Tempelman eqn.	Three-dimensional diffusion (Z1)	$(2/3).(1-\alpha)^{5/3}/[1-(1-\alpha)^{1/3}]$	$[(1-\alpha)^{-1/3}-1]^{2}$
19. Prout-Tompkins eqn.	Branching nuclei (B1)	$\alpha.(1-\alpha)$	$\ln[\alpha.(1-\alpha)^{-1}]$
20. Prout-Tompkins eqn.	Branching nuclei (B2)	$0.5.(1-\alpha).[-\ln(1-\alpha)]^{-1}$	$[-\ln(1-\alpha)]^{2}$
21. Prout-Tompkins eqn.	Branching nuclei (B3)	$(1/3).(1-\alpha).[-\ln(1-\alpha)]^{-2}$	$[-\ln(1-\alpha)]^{3}$
22. Prout-Tompkins eqn.	Branching nuclei (B4)	$(1/4).(1-\alpha).[-\ln(1-\alpha)]^{-3}$	$[-\ln(1-\alpha)]^{4}$

carbonization of cellulosic and lignin components of samples and are given in Tables **3-4**, respectively. The kinetic results given in Tables **3** and **4** indicate that there are variations in the values of Arrhenius parameters (E and log A) depending on the carbonization conditions, calculation method and characteristics of the sample. However, appropriate kinetic models which represent the decomposition of cellulosic and lignin components of biomass samples were not changed, depending on sample characteristics and the method of calculation used.

The most proper kinetic model which represents the carbonization of the cellulosic and lignin ingredients of

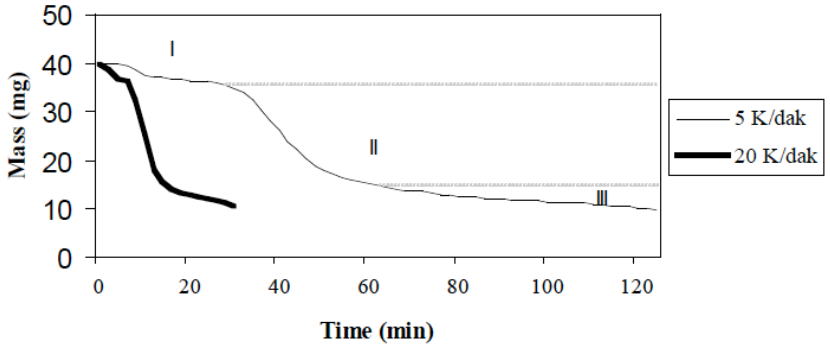

Figure 1: Carbonization TG curves of hazelnut shell at static atmosphere (particle size: 0.250-0.355 mm).

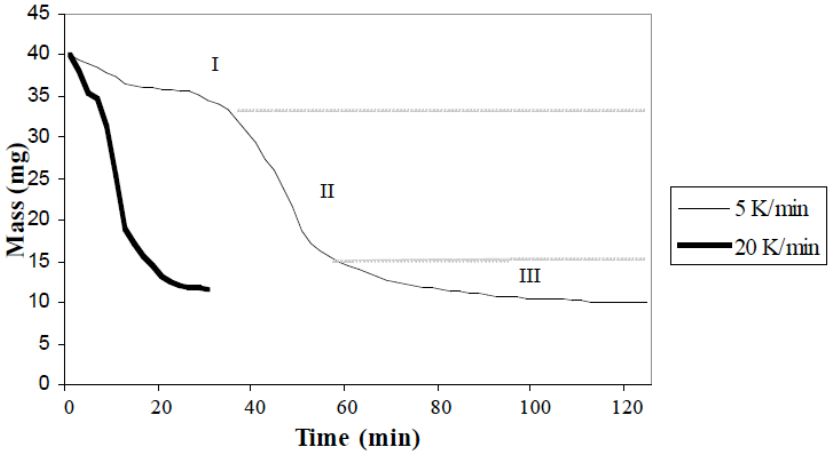

Figure 2: Carbonization TG curves of hazelnut shell at dynamic atmosphere (particle size: 0.250-0.355mm).

all biomass samples were found as $f(\alpha)=(1-\alpha)^2$ and $f(\alpha)=0.5\cdot(1-\alpha)\cdot[-\ln(1-\alpha)]^{-1}$, respectively. Since the slope and the shape of second and third mass loss regions on the TG curves are not the same as each other, the appropriate kinetic models which represent these regions were also found different.

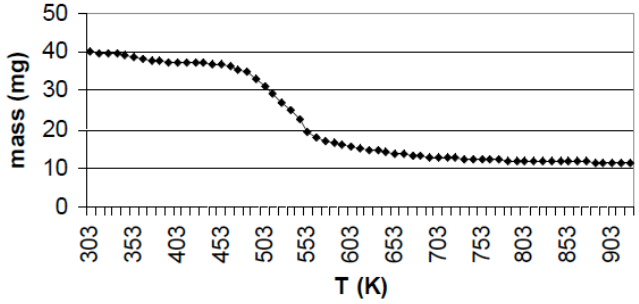

Figure 3: Carbonization TG curve of hazelnut shell at dynamic atmosphere (particle size: 1-1.4 mm; heating rate 5 K/min).

3.1. Effect of the Carbonization Atmosphere on the Kinetic Parameters

As can be seen from the results given in Table **3** that the "E" values obtained for the decomposition of the cellulosic component of the samples at static atmosphere are generally higher than the values obtained in the dynamic atmosphere. Since released gases during the carbonization at static gas atmosphere are not swept by inert gas, the mass transfer resistance and pressure increase and so decomposition is to be harder and activation energy increases. These increases occur linearly with a corresponding increase in "log A" values. This linear relationship between "E" and "log A" has been defined in the literature as the kinetic compensation effect [27, 28]. The results revealed in this work are in agreement with this effect. The effect of carbonization atmosphere on calculated activation energy values for the decomposition lignin component of the samples is not distinctive (Table **4**). This can be explained by the very low gas evolution occurrence during the decomposition of lignin component of the samples.

The existence of an inert sweep gas in the system during carbonization significantly affects the values of the kinetic parameters especially for high heating rates. The reason of this situation is that thermal decomposition of biomass sample gains speed by the

Table 3: Calculated Kinetic Parameters for the Carbonization of Cellulosic Constituents of Biomass Samples

Experiment code	Dharwadkar-Karkhanavala Method				Coats-Redfern Method				Van Krevelen Method			
	E (kJ/mol)	Log A (s^{-1})	f(α)	r	E (kJ/mol)	Log A (s^{-1})	f(α)	r	E (kJ/mol)	Log A (s^{-1})	f(α)	r
H1	45.75	3.90	Fn2	0.99747	47.69	4.23	Fn2	0.99828	51.19	3.50	Fn2	0.99950
H2	45.87	3.92	Fn2	0.99719	45.61	4.14	Fn2	0.99372	50.02	4.25	Fn2	0.99622
H3	44.10	3.31	Fn2	0.99069	43.29	10.35	Fn2	0.97453	52.44	4.28	Fn2	0.98726
H4	38.62	3.23	Fn2	0.99013	30.90	3.94	Fn2	0.97112	35.80	3.31	Fn2	0.98616
H5	52.61	3.98	Fn2	0.99739	67.86	5.17	Fn2	0.99370	76.55	1.93	Fn2	0.99556
A1	49.12	3.94	Fn2	0.99349	63.94	5.12	Fn2	0.99517	70.94	1.92	Fn2	0.99454
A2	48.22	4.44	Fn2	0.99764	45.61	6.05	Fn2	0.99874	50.02	2.57	Fn2	0.99927
A3	44.69	3.17	Fn2	0.99407	50.25	4.30	Fn2	0.98459	58.72	2.60	Fn2	0.99159
A4	38.17	3.12	Fn2	0.99868	38.66	5.67	Fn2	0.99059	42.13	2.52	Fn2	0.99556
A5	56.34	4.37	Fn2	0.99515	65.81	5.13	Fn2	0.99370	75.34	1.93	Fn2	0.99425
G1	36.79	2.50	Fn2	0.99859	36.88	3.62	Fn2	0.99397	44.61	3.51	Fn2	0.99709
G2	50.24	4.68	Fn2	0.99848	36.08	3.55	Fn2	0.99811	36.66	2.61	Fn2	0.99941
G3	53.79	4.11	Fn2	0.99541	36.48	3.52	Fn2	0.97946	43.22	3.14	Fn2	0.99130
G4	36.84	2.20	Fn2	0.99628	24.24	2.78	Fn2	0.99438	31.40	1.75	Fn2	0.99735
G5	60.60	4.68	Fn2	0.99160	53.69	4.32	Fn2	0.99502	58.54	7.95	Fn2	0.99423
C1	37.98	3.00	Fn2	0.99759	42.72	3.99	Fn2	0.99557	47.50	3.99	Fn2	0.99750
C2	42.20	4.44	Fn2	0.97360	37.41	4.35	Fn2	0.97651	39.08	3.75	Fn2	0.98003
C3	40.12	2.86	Fn2	0.98246	38.14	3.70	Fn2	0.99537	43.97	3.47	Fn2	0.99788
C4	37.98	2.63	Fn2	0.99449	35.03	3.54	Fn2	0.98255	43.16	3.42	Fn2	0.99172
C5	45.69	3.46	Fn2	0.99428	37.24	3.66	Fn2	0.98040	44.97	3.61	Fn2	0.99132

increasing heating rate and the release of the volatile matter increases. At high heating rates the amount of the volatile matters in the carbonization atmosphere increases and the sweep effect of the inert sweep gas reflects in a more effective way to kinetic parameters [29, 30]. If the carbonization is conducted at dynamic atmosphere, the concentration of volatile matters in the carbonization atmosphere decreases and the effects of mass transfer that prevents the release of volatile matter decreases [30].

3.2. Effect of the Heating Rate on the Kinetic Parameters

It is clear from the results presented in Tables **3** and **4** that the “E” and “log A” values obtained for the decomposition of cellulosic and lignin components of biomass samples at the heating rate of 5 K/min are generally higher than the values obtained at the heating rate of 20 K/min.

As can be seen from Figure **1** the thermal decomposition of biomass sample accelerated with increasing heating rate and in parallel to decomposition, the rate of volatile matter evolution increased. It was reported that an increase in heating rate during a thermal decomposition cause to decrease the restricted effects of mass transfer [31-33]. The results of the studies given in the literature showed that; system design, crucible of sample, furnace wall thickness and furnace material can cause changes on the effect of heating rate on the activation energy [3,12,34]. Besides, it is indicated that the value of the pre-exponential factor decreases with increasing heating rate [3]. In this case, considering the kinetic compensation effect, "log A" and "E" values can be thought to differ in parallel way.

At high heating rates, temperature gradient develops especially in the samples which have weak thermal conductivity such as wood, thus the decomposition reactions are controlled by heat transfer

Table 4: Calculated Kinetic Parameters for the Carbonization of Lignin Constituents of Biomass Samples

Experiment code	Dharwadkar-Karkhanavala Method				Coats-Redfern Method				Van Krevelen Method			
	E (kJ/mol)	Log A (s^{-1})	f(α)	r	E (kJ/mol)	Log A (s^{-1})	f(α)	r	E (kJ/mol)	Log A (s^{-1})	f(α)	r
H1	41.69	2.68	B2	0.98563	9.20	1.87	B2	0.97302	12.18	0.16	B2	0.99279
H2	37.53	2.94	B2	0.98951	7.05	2.31	B2	0.97198	10.28	0.28	B2	0.99494
H3	41.48	2.36	B2	0.98766	19.70	2.65	B2	0.98870	23.45	1.28	B2	0.99298
H4	59.75	3.54	B2	0.99856	24.71	2.90	B2	0.98616	30.93	1.82	B2	0.99670
H5	48.58	3.20	B2	0.99128	19.75	2.66	B2	0.99358	22.28	1.09	B2	0.99636
A1	35.97	2.25	B2	0.99589	13.06	2.20	B2	0.99725	15.72	0.34	B2	0.99896
A2	30.87	1.63	B2	0.99803	13.33	2.24	B2	0.99590	16.58	0.48	B2	0.99910
A3	39.70	2.48	B2	0.97138	11.98	2.23	B2	0.94725	14.62	0.45	B2	0.98143
A4	36.18	2.65	B2	0.98462	11.39	2.76	B2	0.96844	14.74	1.00	B2	0.99009
A5	52.88	3.81	B2	0.99649	19.24	2.67	B2	0.99.497	20.85	1.04	B2	0.99844
G1	57.70	4.50	B2	0.98296	16.45	2.38	B2	0.98151	17.46	0.41	B2	0.99087
G2	47.60	3.54	B2	0.98703	11.87	2.71	B2	0.93280	14.98	0.82	B2	0.98502
G3	33.95	1.51	B2	0.97601	15.37	2.38	B2	0.95020	19.08	0.73	B2	0.98042
G4	30.02	1.24	B2	0.99519	13.63	2.27	B2	0.98837	17.38	0.56	B2	0.99750
G5	52.75	3.25	B2	0.99178	21.60	2.68	B2	0.98891	23.99	1.07	B2	0.99528
C1	43.26	2.68	B2	0.99821	14.55	3.48	B2	0.99361	18.14	0.40	B2	0.99905
C2	51.59	2.15	B2	0.99628	15.39	3.15	B2	0.97432	24.16	0.90	B2	0.99213
C3	50.10	2.93	B2	0.99668	17.99	2.48	B2	0.98092	22.16	0.89	B2	0.99498
C4	49.40	3.65	B2	0.99511	15.35	2.31	B2	0.96990	17.23	0.39	B2	0.99244
C5	42.76	2.63	B2	0.99702	16.90	2.44	B2	0.99768	19.92	0.75	B2	0.99947

mechanisms rather than chemical kinetics. Therefore, it is recommended to perform experiments at relatively low heating rates for the kinetic studies [35].

3.3. Effect of Particle Size on the Kinetic Parameters

One of the most important parameters affecting the thermal decomposition processes is particle size of the sample. Large-scale particles are hard to degrade completely and so, more time can be required, because thermal decomposition moves from the particle surface to particle's center. Heating of small particles becomes more uniform with the decrease of particle size and so, reduction occurs in the effects of heat and mass transfer resistance. When the particle size becomes smaller, degradation temperature drops and as a result, activation energy decreases [22,36,37]. It can be seen from the results given in Table **3** that the "E" and "log A" values obtained for the carbonization of the cellulosic component of coarse grained biomass samples are generally higher than the "E" and "log A" values obtained for the fine grained samples. The "E" values calculated for the carbonization of lignin component of the samples are also increased with the increasing particle size of the samples except chestnut shell sample. Different physical appearance and shape of the raw material in comparison with other biomass samples can be the reason of the difference observed in the activation energies of chestnut shell sample. Unlike the granular shape and appearance of apricot stone, hazelnut shell and grapeseed, the shape of chestnut shell is resembling spongy in appearance. Although not effective in the second decomposition region, the physical texture of the chestnut shell is more effective than its particle size in the third decomposition region. It can be said that its external surface area can be larger than granular particle-shaped biomass samples, due to its coarse particles (pulverized) is more flat and thin. Larger external surface area may facilitate decomposition during high temperature carbonization and so, "E" value decreased.

4. CONCLUSIONS

The kinetic parameters and best fitting model equations for the carbonization of cellulosic and lignin components of apricot stone, hazelnut shell, grapeseed and chestnut shell, were determined by using three different calculation methods and 22 different model equations. It was concluded that the Arrhenius Parameters (E and log A) were changed depending on carbonization conditions, the method of calculation used and the type of biomass sample. Calculated "E" and "log A" values for the carbonization of hemicellulose and cellulose components of biomass samples were found higher than those calculated for the carbonization of the lignin components of biomass samples.

REFERENCES

[1] Vuthaluru HB. Thermal Behaviour of Coal/Biomass Blends During Co-Pyrolysis. Fuel Process Technol 2003; 85: 141-155. http://dx.doi.org/10.1016/S0378-3820(03)00112-7

[2] Kissenger HE. Reaction Kinetics In DTA. Anal Chem 1957; 29: 1702-1706.

[3] Wentlandt WW. Thermal Analysis, 3rd ed. John Wiley and Sons Inc.: New York 1986.

[4] Orfao JJM, Antunes FJA, Figueiredo JL. Pyrolysis Kinetics of Lignocellulosic Materials-Three Independent Reactions Model. Fuel 1999; 78: 349-358. http://dx.doi.org/10.1016/S0016-2361(98)00156-2

[5] Yang H, Yan R, Chen H, Lee DH, Zheng C. Characteristics of Hemicellulose, Cellulose And Lignin Pyrolysis. Fuel 2007; 86: 1781-1788. http://dx.doi.org/10.1016/j.fuel.2006.12.013

[6] Antal MJ, Varhegyi G. Cellulose Pyrolysis Kinetics: The Current State of Knowlodge. Ind Eng Chem Res 1995; 34: 703-717. http://dx.doi.org/10.1021/ie00042a001

[7] Milosavljevic I, Suuberg EM. Cellulose Thermal Decomposition Kinetics: Global Mass Loss Kinetics. Ind Eng Chem Res 1995; 34: 1081. http://dx.doi.org/10.1021/ie00043a009

[8] Orfao JJM, Figueiredo F. A Simplified Merhod For Determination of Lignocellulosic Materials Pyrolysis Kinetics From Isothermal Thermogravimetric Experiments. Thermochim Acta 2001; 380: 67-78. http://dx.doi.org/10.1016/S0040-6031(01)00634-7

[9] Hagedorn MM, Bockhorn H, Krebs L, Müller U. A Comparative Kinetic Study on the Pyrolysis of Three Different Wood Species. J Anal Appl Pyrol 2003; 68: 231-249. http://dx.doi.org/10.1016/S0165-2370(03)00065-2

[10] Sharma A, Rao TR. Kinetics of Pyrolysis of Rice Husk. Bioresource Technol 1999; 67: 53-59. http://dx.doi.org/10.1016/S0960-8524(99)00073-5

[11] Balcı S, Doğu T, Yücel H. Pyrolysis Kinetics of Lignocellulosic Materials. Ind Eng Chem Res 1993; 32: 2573-2579. http://dx.doi.org/10.1021/ie00023a021

[12] Gonzalez JF, Encinar JM, Canito JL, Sabio E, Chacon M. Pyrolysis of Cherry Stones: Energy Uses of the Different Fractions And Kinetic Study. J Anal Appl Pyrol 2003; 67: 165-190. http://dx.doi.org/10.1016/S0165-2370(02)00060-8

[13] Vamvuka D, Troulinos S, Kastanaki E. The Effect of Mineral Matter on the Physical And Chemical Activation of Low Rank Coal And Biomass Materials. Fuel 2006; 85: 1763-1771. http://dx.doi.org/10.1016/j.fuel.2006.03.005

[14] Wang J, Wang G, Zhang M, Chen M, Li D, Min F, Chen M, Zhang S, Ren Z, Yan Y. A Comparative Study of Thermolysis Characteristics And Kinetics of Seaweeds And Firwood. Process. Biochem 2006; 41: 1883-1886. http://dx.doi.org/10.1016/j.biochi.2006.07.017

[15] Sait HH, Hussain A, Salema AA, Ani FN. Pyrolysis And Combustion Kinetics of Date Palm Biomass Using Thermogravimetric Analysis. Bioresource Technology 2012; 118: 382-389. http://dx.doi.org/10.1016/j.biortech.2012.04.081

[16] Reschmeier R, Roveda D, Müller D, Karl J. Pyrolysis Kinetics of Wood Pellets In Fluidized Beds. Journal of Analytical and Applied Pyrolysis 2014; 108: 117-129. http://dx.doi.org/10.1016/j.jaap.2014.05.009

[17] Ceylan S, Topçu Y. Pyrolysis Kinetics of Hazelnut Husk Using Thermogravimetric Analysis. Bioresource Technology 2014; 156: 182-188. http://dx.doi.org/10.1016/j.biortech.2014.01.040

[18] Flynn JH, Wall LA. General Treatment of the Thermogravimetry of Polymers. J Res Nat Bur Stand 1966; 70: 487-489. http://dx.doi.org/10.6028/jres.070A.043

[19] Keattch CJ, Dollimore D. An Introduction To Thermogravimetry, 2nd ed. Heyden: London 1975.

[20] Ozawa T. A New Method of Analyzing Thermogravimetric Data. B Chem Soc Jpn 1965; 38: 1881-1886. http://dx.doi.org/10.1246/bcsj.38.1881

[21] Doyle CD. Series Approximations to the Equation of Thermogravimetric Data. J Nature 1965; 207: 290-291. http://dx.doi.org/10.1038/207290a0

[22] Coats AW, Redfern JP. Kinetic Parameters from Thermogravimetric Data. J Nature 1964; 201: 68. http://dx.doi.org/10.1038/201068a0

[23] Horowitz HH, Metzger G. A New Analysis of Thermogravimetric Traces. Anal Chem 1923; 35: 1464-1468. http://dx.doi.org/10.1021/ac60203a013

[24] Ozawa T. Kinetic Analysis of Derivative Curves in Thermal Analysis. J Therm Anal 1970; 2: 301-324. http://dx.doi.org/10.1007/BF01911411

[25] Dharwadkar SR, Karkhanavala MD. Calculation of Activation Energy of Decomposition Reactions from Thermogravimetric Analysis. Therm Anal 1969; 2: 1049-1059. http://dx.doi.org/10.1016/B978-0-12-395734-4.50031-X

[26] Van Krevelen DW, Van Heerden C, Huntjens FJ. Physicochemical Aspects of the Pyrolysis of Coal and Related Organic Compounds. Fuel 1951; 30: 253-258.

[27] Garn PD. An Examination of the Kinetic Compensation Effect. J Therm Anal 1975; 7: 475-478. http://dx.doi.org/10.1007/BF01911956

[28] Mericboyu AE, Küçükbayrak S. Kinetic Analysis of Non-Isothermal TG Curves of Natural Turkish Dolomites. Thermochim Acta 1994; 232: 225-232. http://dx.doi.org/10.1016/0040-6031(94)80062-6

[29] Koçkar OM, Onay O, Pütün AE, Pütün E. Fixed Bed Pyrolysis of Hazelnut Shell: A Study on the Mass Transfer Limitations on Product Yields and Characterization of the Pyrolysis Oil. Energ Sources 2000; 22: 913-924. http://dx.doi.org/10.1080/00908310051128291

[30] Zaror CA, Pyle DL. The Pyrolysis of Biomass: A General Review, P. Indian. Acad Sci (Eng Sci) 1982; 5: 269-85.

[31] Demirbaş A. Determination of Calorific Values of Bio-Chars and Pyro-Oils from Pyrolysis of Beech Trunkbarks. Anal Appl Pyrol 2004; 72: 215-219. http://dx.doi.org/10.1016/j.jaap.2004.06.005

[32] Seebauer V, Petek J, Standinger G. Effect of Particle Size, Heating Rate And Pressure on Measurement of the Pyrolysis Kinetics By Thermogravimetric Analysis. Fuel 1997; 76(13): 1277-1282. http://dx.doi.org/10.1016/S0016-2361(97)00106-3

[33] Katyal S. Carbonisation of Bagasse In A Fixed Bed Reactor: Influence of Process Variables on Char Yield And Characteristics. Renew Energ 2003; 28: 713-725. http://dx.doi.org/10.1016/S0960-1481(02)00112-X

[34] Tsamba AJ, Yang W, Blasiak W. Pyrolysis Characteristics and Global Kinetics of Coconut And Cashew Nut Shells. Fuel Process Technol 2006; 87(6): 523-530. http://dx.doi.org/10.1016/j.fuproc.2005.12.002

[35] Reina J, Velo E, Puigjaner L. Thermogravimetric Study of the Pyrolysis of Waste Wood. Thermochim Acta 1998; 320: 161-167. http://dx.doi.org/10.1016/S0040-6031(98)00427-4

[36] Gao X, Chen D, Dollimore D. The Effect of the Reaction Heat on Kinetic Analysis By TG Under a Rising Temperature Program. Thermochim Acta 1993; 215: 83-95. http://dx.doi.org/10.1016/0040-6031(93)80083-M

[37] Özyurtkan, MH, Özçimen D, Ersoy-Meriçboyu A. Investigation of the carbonization behavior of hybrid poplar. Fuel Process Technol 2008; 89(9): 858-863.

Received on 17-07-2014 Accepted on 26-08-2014 Published on 23-11-2014

DOI: http://dx.doi.org/10.15377/2409-983X.2014.01.01.2